NASA TECHNICAL NOTE

NASA TN D-5468

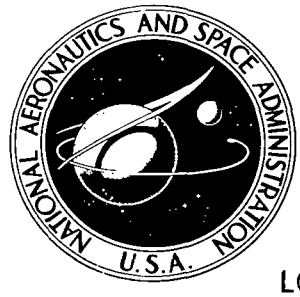

LARGE-SCALE WIND-TUNNEL INVESTIGATION OF AN M1-L LIFTING BODY WITH AN INFLATABLE AND A RIGID AFTERBODY

by
Kenneth W. Mort
Ames Research Center
and
Michael D. Falarski
Army Aeronautical Research Laboratory

NATIONAL AERONAUTICS AND SPACE ADMINISTRATION • WASHINGTON, D. C. • OCTOBER 1969

1. Report No.	2. Government Accession No.	3. Recipient's Catalog No.
NASA TN D-5468		

4. Title and Subtitle
LARGE-SCALE WIND-TUNNEL INVESTIGATION OF AN M1-L LIFTING BODY WITH AN INFLATABLE AND A RIGID AFTERBODY

5. Report Date
October 1969

6. Performing Organization Code

7. Author(s)
Kenneth W. Mort and Michael D. Falarski

8. Performing Organization Report No.
A-2894

9. Performing Organization Name and Address
NASA Ames Research Center
and
Army Aeronautical Research Laboratory
Moffett Field, Calif. 94035

10. Work Unit No.
124-07-02-16-00-21

11. Contract or Grant No.

13. Type of Report and Period Covered
TECHNICAL NOTE

12. Sponsoring Agency Name and Address
NATIONAL AERONAUTICS AND SPACE ADMINISTRATION
Washington, D. C., 20546

14. Sponsoring Agency Code

15. Supplementary Notes

16. Abstract

The M1-L lifting body concept employs a high volumetric efficiency forebody and an inflatable afterbody that is deployed to provide lift-to-drag ratios sufficient for horizontal landings. The purpose of the investigation described here was to determine the low-speed aerodynamic characteristics of a large-scale model with an inflatable afterbody. In addition, a model with a rigid afterbody was tested as a datum for aeroelastic characteristics.

Deployment of the inflatable afterbody increased the maximum lift-to-drag ratio (L/D) from less than 1 to slightly more than 2. This value was about 15 to 20 percent less than that for the model with the rigid afterbody. Because a maximum L/D of about 2-1/2 is the minimum value required to accomplish a horizontal landing, this 20-percent reduction appeared to be the most significant effect of flexibility.

Studies indicated that deployment of the inflatable afterbody is mechanically feasible.

17. Key Words (Suggested by Author(s))	18. Distribution Statement
Lifting body Inflatable afterbody Subsonic aerodynamics, aircraft Subsonic aerodynamics, missiles and space vehicles	Unclassified - Unlimited

19. Security Classif. (of this report)	20. Security Classif. (of this page)	21. No. of Pages	22. Price*
Unclassified	Unclassified	10	$3.00

*For sale by the Clearinghouse for Federal Scientific and Technical Information
Springfield, Virginia 22151

LARGE-SCALE WIND-TUNNEL INVESTIGATION OF AN M1-L LIFTING BODY WITH AN INFLATABLE AND A RIGID AFTERBODY

By Kenneth W. Mort
Ames Research Center

and

Michael D. Falarski
Army Aeronautical Research Laboratory

SUMMARY

The M1-L lifting body concept employs a high volumetric efficiency forebody and an inflatable afterbody that is deployed to provide lift-to-drag ratios sufficient for horizontal landings. The purpose of the investigation described here was to determine the low-speed aerodynamic characteristics of a large-scale model with an inflatable afterbody. In addition, a model with a rigid afterbody was tested as a datum for aeroelastic characteristics.

Deployment of the inflatable afterbody increased the maximum lift-to-drag ratio (L/D) from less than 1 to slightly more than 2. This value was about 15 to 20 percent less than that for the model with the rigid afterbody. Because a maximum L/D of about 2-1/2 is the minimum value required to accomplish a horizontal landing, this 20-percent reduction appeared to be the most significant effect of flexibility.

Studies indicated that deployment of the inflatable afterbody is mechanically feasible.

INTRODUCTION

Many studies have been conducted in developing lifting body reentry configurations capable of gliding to a specified recovery site and making a conventional horizontal landing. One such concept is referred to as the M1-L lifting-body configuration. A high volumetric efficiency forebody (30° half-cone) is used as the prime space vehicle, and an inflatable afterbody is deployed at low speeds to provide adequate lift-to-drag ratios for performing the landing maneuver. Several small-scale investigations examined the aerodynamic characteristics of the reentry configuration, or forebody, and are reported in references 1 through 9. To investigate the aerodynamic characteristics of the concept with the inflatable afterbody, two large-scale models were constructed: a model with an inflatable afterbody that could be used for both steady-state aerodynamic measurements and deployment investigations, and a model with a rigid afterbody used as a datum for aeroelastic characteristics. Tests of these models were performed in the Ames 40- by 80-Foot Wind Tunnel, and the results are presented herein.

NOTATION

b maximum span, 13.4 ft

C_D drag coefficient, $\frac{D}{qS}$

C_L lift coefficient, $\frac{L}{qS}$

C_l rolling-moment coefficient, $\frac{\text{rolling moment}}{qSb}$

C_y side-force coefficient, $\frac{\text{side force}}{qS}$

C_m pitching-moment coefficient, $\frac{\text{pitching moment}}{qS\ell}$

C_n yawing-moment coefficient, $\frac{\text{yawing moment}}{qSb}$

D drag force, lb

ℓ overall length of model with afterbody, 14.1 ft

L lift force, lb

q free-stream dynamic pressure, psf

r radial distance from cone axis (see fig. 3), in.

R Reynolds number, $\frac{V\ell}{\text{kinematic viscosity}}$

S reference area (body planform area with afterbody), 142 ft^2

V free-stream velocity, fps

x distance from leading edge (see fig. 3), in.

y distance above cone axis, along axis (see fig. 3), in.

α angle of attack (see fig. 3), deg

δ_f flap deflection (see fig. 3), deg

δ_r rudder deflection, both sides are moved together (see fig. 3), deg

Δp_c internal pressure of inflatable afterbody cavity referenced to atmospheric pressure, psi

Δp_i internal pressure of primary structure referenced to atmospheric pressure, psi

The forces and moments developed by the model were resolved along the wind axis.

MODEL DESCRIPTION

Photographs of the models installed in the test section of the Ames 40- by 80-Foot Wind Tunnel are shown in figure 1. Photographs showing the model with the inflatable afterbody in various stages of assembly are shown in figure 2. Basic model dimensions and geometry are presented in figure 3 and table I.

The model with the inflatable afterbody was constructed by Goodyear Aerospace Corporation. The primary structure of the inflatable afterbody was made of Goodyear Airmat.[1] This structure included the upper surface, the rear surface, the fins and control surfaces, and the internal vertical members. The catenary and remaining afterbody exterior were rubberized fabric (see figs. 2(b), 2(c), and 3). Further details of the design and construction are given in reference 10. The primary structure was inflated with air at 5 to 25 psi, and the interior of the afterbody or cavity was inflated with air at 0.1 to 0.2 psi.

TEST PROCEDURE

The tests were performed by varying angle of attack for various internal pressures, free-stream dynamic pressures, and control settings.

Deployment testing was performed at dynamic pressures of 24 and 62 psf. The procedure involved releasing the harness that restrained the deflated afterbody, inflating the primary structure with high pressure air contained in compressed air bottles in the forebody, and inflating the afterbody cavity with ram air from the scoop on the lower surface of the forebody (see fig. 3). Signals from pressure sensors in the cavity actuated a drive system to open and close the scoop automatically to regulate the cavity pressure. During the steady-state testing, this scoop was closed to provide more uniform cavity pressure (supplied from an external source) and to eliminate the random flow effects that would appear as scatter in the data from the aperiodic opening and closing of the scoop.

[1]Trademark, Goodyear Aerospace Corporation, Akron, Ohio.

REDUCTION OF DATA

Corrections

No tunnel-wall corrections were applied to the data presented because estimates indicated that such effects on the data were well within the indicated accuracy.

The data were corrected for tares obtained for the unshielded struts. These tares were obtained without the models and hence are subject to errors from differences due to interaction with the models. However, experience with other models using these same struts indicates that the interference effects are small.

Accuracy of Measurements

The various quantities measured in the wind tunnel were accurate within the following limits. The values given include error limits due to calibrations, corrections, and recording methods. The force pressure, and moment measurements for each data point were obtained by averaging 10 samples. Hence, the accuracy limits listed for these items are for the average values.

Angle of attack	±0.3°
Lift	±10 lb
Drag	±3 lb
Side force	±3 lb
Pitching moment	±300 ft-lb
Rolling moment	±400 ft-lb
Yawing moment	±100 ft-lb
Free-stream dynamic pressure	±0.5 percent above 20 psf, ±0.1 psf below 20 psf
Primary-structure pressure	±0.5 psi
Cavity pressure	±0.02 psi
Control surface settings	±2°

RESULTS

Table II is a complete index to the figures which show the test results. Basic longitudinal aerodynamic characteristics are presented in figures 4 through 10. Results are shown in figure 4 with the afterbody off and in figures 5 through 9 with the inflatable afterbody on. Data for several inflation pressures and dynamic pressures are presented. Figure 10 shows results for the rigid model. Longitudinal aerodynamic characteristics with and without the afterbodies are summarized in figure 11. A comparison of the results for the inflatable and rigid model is presented in figure 12. In figure 13 photographs of the model with the inflatable afterbody show the deflection of the afterbody during testing. Longitudinal and directional control effectiveness data are presented in figures 14 and 15, respectively, for both models. Photographs of various stages of the deployment of the inflatable afterbody are shown in figure 16. The results shown in figures 11 through 16 will be discussed in the next section.

DISCUSSION

The Effects of the Inflatable Afterbody

As stated in the introduction the purpose of the inflatable afterbody was to improve the longitudinal aerodynamic characteristics of the forebody sufficiently to allow a horizontal landing. To examine this improvement, figure 11 is presented showing the aerodynamic characteristics of the forebody with and without the inflatable afterbody.[2] It is evident from this figure that the inflatable afterbody significantly improved the aerodynamic characteristics of the model. The lift curve slope was increased from about 0.012 to about 0.027 per degree, drag coefficient at zero lift was reduced from 0.32 to 0.12, and the static margin went from 0.1045 to -0.110 (at $C_m = 0$). Maximum L/D, which is probably the most important parameter, was increased from less than 1 to somewhat over 2. As indicated by several other studies (e.g., ref. 11), a maximum L/D of 2-1/2 is about the minimum value required for horizontal landing capability.

Afterbody Flexibility

The aerodynamic characteristics are shown in figure 11 for the model with the inflatable afterbody at an inflation pressure of 10 psi in the primary structure, a longitudinal control setting of -30°, and a free-stream dynamic pressure of 50 psf. Variations in these parameters would be expected to affect the aerodynamic characteristics because of afterbody flexibility. To examine this, results are shown in figure 12 for several inflation pressures and control settings; the dynamic pressure is 25 psf. Results for the

[2]These data were obtained from figures 4 and 9.

model with the rigid afterbody are also shown.[3] It is evident that lift-curve slope and stability vary with internal pressure and flap setting. Differences between the two models are also evident. The L/D does not appear to vary appreciably with pressure; however, it is always lower for the model with the inflatable afterbody - the maximum value is about 20 percent lower. The reasons for this can be seen in photographs in figure 13. As can be seen, there were wrinkles along the side and bulging of the lower surface near the juncture of the forebody and afterbody that caused the drag to be higher.[4] (The minimum drag coefficient was about 50 percent higher.)

The effect of dynamic pressure on afterbody flexiblity was compared for the two models with the controls on at various dynamic pressures. Increasing the dynamic pressure from 25 to about 50 psf (maximum for which comparisons could be made) did not significantly change the incremental differences between the inflatable and rigid models at primary structure pressures equal to or greater than 10 psi. (For this reason, the internal pressure of the primary structure was not made dimensionless with dynamic pressure.) Decreasing the dynamic pressure below 25 psf also did not significantly change the incremental differences between the two models but showed large variations in aerodynamic characteristics due to flow characteristics sensitive to Reynolds number (see, e.g., figs. 5(a) and 10).

Control Effectiveness

The longitudinal control effectiveness of the two models is presented in figure 14. The control effectiveness of the inflatable model was less than that of the rigid model (15 to 30 percent depending on the angle of attack and dynamic pressure). This difference could be due to deflection of the inflatable control surfaces, although it should be pointed out that the controls were different: the hinge line was sealed for the inflatable controls and not sealed for the rigid controls. (The evident nonlinearity from 0° to -10° deflection occurred for the rigid controls as well as for the inflatable controls and hence appears to be due mainly to the control system configuration.)

Directional control effectiveness for the two models was significantly different. As shown in figure 15 the control effectiveness of the inflatable model appears to be nonlinear, whereas that of the rigid model is essentially linear. At rudder deflections greater than 10° the inflatable model appears to have higher control effectiveness than the rigid model. Again, the hinge line was sealed for the inflatable control surfaces and not for the rigid control surfaces.

---

[3]These results were determined from the data of figures 5, 7, 9, 10, and 14; some minor extrapolation was required.

[4]The wrinkles and bulging appear the same as were evident in figure 1, which were due to drooping of the afterbody about the upper-surface intersection of the forebody and afterbody because of its own weight.

Deployment

Deployment of the inflatable afterbody was studied to establish the mechanical feasibility. Two deployment sequences are shown in figure 16. The first deployment was made at a dynamic pressure of 24 psf (fig. 16(a)). The primary structure was fully inflated in about 10 seconds; however, the cavity did not inflate as rapidly as was intended because the scoop on the bottom of the forebody (see fig. 3), which was the ram air inlet for the cavity, did not function properly. The second deployment was made at a dynamic pressure of 62 psf (fig. 16(b)). During this deployment the cavity inflation system operated properly, and the cavity was completely inflated in about 3 seconds; but the high pressure system that inflates the primary structure failed to operate, hence, it was not inflated.

Even though the primary structure and cavity were not inflated simultaneously during either deployment, it is apparent from the photographs of figure 16 that the shape of the fins was good in one deployment and that the shape of the afterbody was good in the other. This suggests that deployment of the inflatable afterbody is mechanically feasible and would have been successful if both inflation systems had operated simultaneously.

CONCLUDING REMARKS

Deployment of the inflatable afterbody increased the maximum L/D from less than 1 to slightly more than 2. As indicated by several studies (see, e.g., ref. 11) a maximum L/D of 2-1/2 is about the minimum value required for a horizontal landing. Hence, the maximum L/D of the model with the inflatable afterbody is too low. The maximum L/D for the model with the rigid afterbody is only about 2-3/4, which is near the minimum required for a horizontal landing.

The maximum L/D for the model with the inflatable afterbody is about 15 to 20 percent lower than that of the rigid model because of increased drag caused by bulging, wrinkles, etc. The bulging and wrinkles depend on the design and materials; however, any inflatable structure will probably have higher drag than a rigid structure. Hence, it is necessary to use body shapes with sufficiently high maximum L/D to allow for losses due to flexibility. It is apparent that the M1-L configuration does not have sufficiently high L/D.

Deployment of the inflatable afterbody was considered mechanically feasible. Operational problems were encountered during deployment studies, but these problems were not related to the configuration or to the method of deployment.

Ames Research Center
National Aeronautics and Space Administration
Moffett Field, Calif., 94035, June 12, 1969

REFERENCES

1. Eggers, Alfred J., Jr.; and Wong, Thomas J.: Re-entry and Recovery of Near-Earth Satellites, With Particular Attention to a Manned Vehicle. NASA MEMO 10-2-58A, 1958.

2. Savage, Howard F.; and Tinling, Bruce E.: Subsonic Aerodynamic Characteristics of Several Blunt, Lifting Atmospheric-Entry Shapes. NASA MEMO 12-24-58A, 1959.

3. Hassell, James L., Jr.: Investigation of the Low-Subsonic Stability and Control Characteristics of a 1/3-Scale Free-Flying Model of a Lifting-Body Reentry Configuration. NASA TM X-297, 1960.

4. Dennis, David H.; and Edwards, George G.: The Aerodynamic Characteristics of Some Lifting Bodies. NASA TM X-376, 1960.

5. Sarabia, Michael F.: Aerodynamic Characteristics of Blunt Half-Cone Entry Configuration at Mach Numbers From 3 to 6. NASA TM X-393, 1960.

6. Tunnell, Phillips J.: The Static and Dynamic Stability Derivatives of a Blunt Half-Cone Entry Configuration at Mach Numbers From 0.70 to 3.50. NASA TM X-577, 1961.

7. DeRose, Charles E.: The Aerodynamic Characteristics of a Blunt Half-Cone Entry Configuration Obtained From Ballistic Range Tests at Mach Numbers Near 3. NASA TM X-578, 1961.

8. Holtzclaw, Ralph W.: Static Stability and Control Characteristics of a Half-Cone Entry Configuration at Mach Numbers From 2.2 to 0.7. NASA TM X-649, 1962.

9. Holdaway, George H.; Polek, Thomas E.; and Kemp, Joseph H., Jr.: Aerodynamic Characteristics of a Blunt Half-Cone Entry Configuration at Mach Numbers of 5.2, 7.4, and 10.4. NASA TM X-782, 1963.

10. Anon.: M-1-L Re-entry Vehicle (Wind Tunnel Model, Full-Scale) Design, Fabrication, and Testing. Final Report, 10 Aug. 1962 - 15 Nov. 1963, Goodyear Aerospace Corporation Report Number GER-11141, (NASA Contract NAS 2-1037), NASA CR-53716, 1964.

11. Hoey, Robert G.: Horizontal Landing Techniques for Hypersonic Vehicles. AGARD Rep. 428, Jan. 1963.

TABLE I.- BODY COORDINATES
(See fig. 3)

x, in.	y, in.	r, in.
0	0	0
.44		4.95
1.66		9.55
2.20		10.91
3.13		12.75
4.08		14.26
7.83		18.70
11.40	16.40	
12.52		22.62
18.80		26.88
25.06		30.70
28.20		32.54
77.00	23.83	
77.55	23.97	
81.08	24.25	
84.60	24.32	
88.12	24.18	
91.65	23.90	
93.90	23.62	70.50
98.70	22.84	72.76
105.75	20.94	75.58
112.80	18.54	77.48
119.85	15.37	78.75
130.42	9.52	80.02
141.00	2.04	80.44
151.58	-6.56	80.23
162.15	-15.65	79.66
169.50	-22.28	79.10

Circular

Straight line

Conical section

TABLE II.- INDEX TO FIGURES

Afterbody configuration	Type of data	q, psf	Δp_i, psi	Δp_c, psi	δ_f, deg	Figure
Off	Longitudinal	50			Off	4
Inflatable	Longitudinal	5,25	5	0.2	Off	5(a)
		10-33	10	.2	Off	5(b)
		10-33	15	.2	Off	5(c)
		15	15	.1	Off	5(d)
				.2		
Inflatable with controls	Longitudinal	30-70	15	.2	0	6
		30,50	10,15	.2	-10	7(a)
		15	5,10,15	.2	-10	7(b)
		30,50	10,15	.1	-10	7(c)
		30,50	15	.2	-20	8
		30,50	10,15	.2	-30	9
Rigid	Longitudinal	5-50			Off	10
Off and inflatable	Longitudinal comparison	50	10	.2	-30	11
Inflatable and rigid		25	5,10,15	.2	Off, -10,-30	12
Inflatable with controls	Photos of deflection	29	15	.2	-30	13
Inflatable	Longitudinal control effectiveness	30,50	15	.2	Vary	14
Rigid		25,50				
Inflatable	Directional control effectiveness	28,48	15	.2	0	15
Rigid		48				
Inflatable	Deployment	24,62	Vary	Vary	Off	16

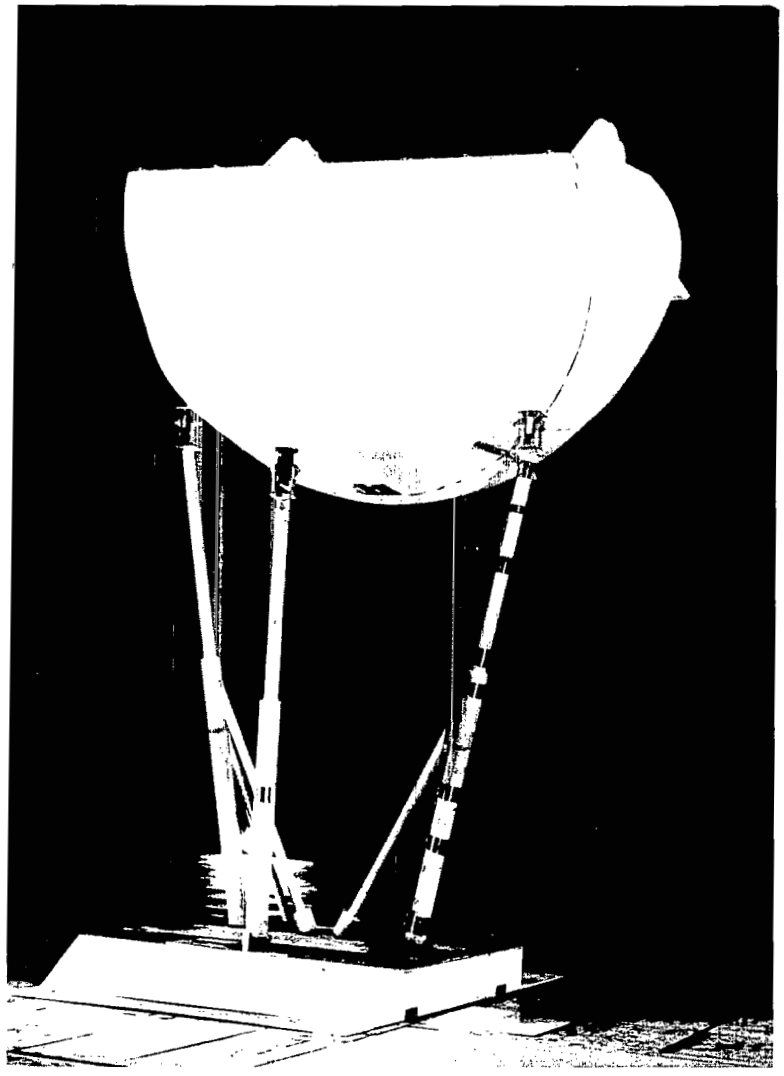

A-35755.1

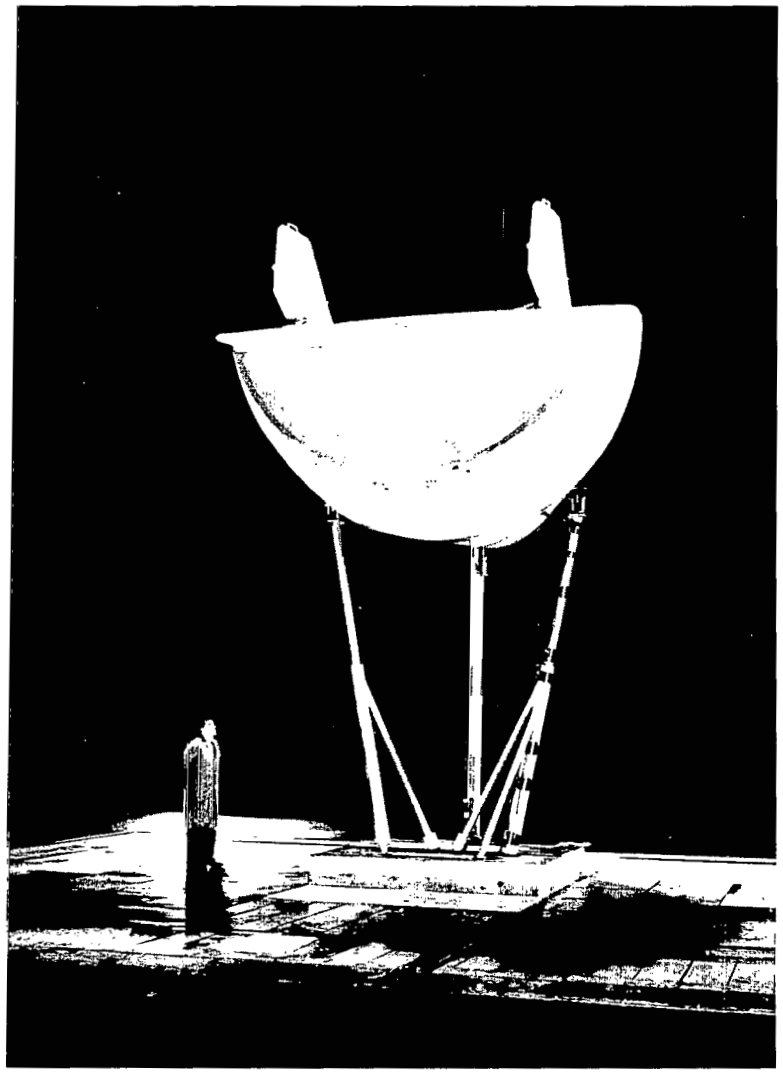

A-35756.1

(a) Model with inflatable afterbody.

Figure 1.- M1-L mounted in the Ames 40- by 80-Foot Wind Tunnel.

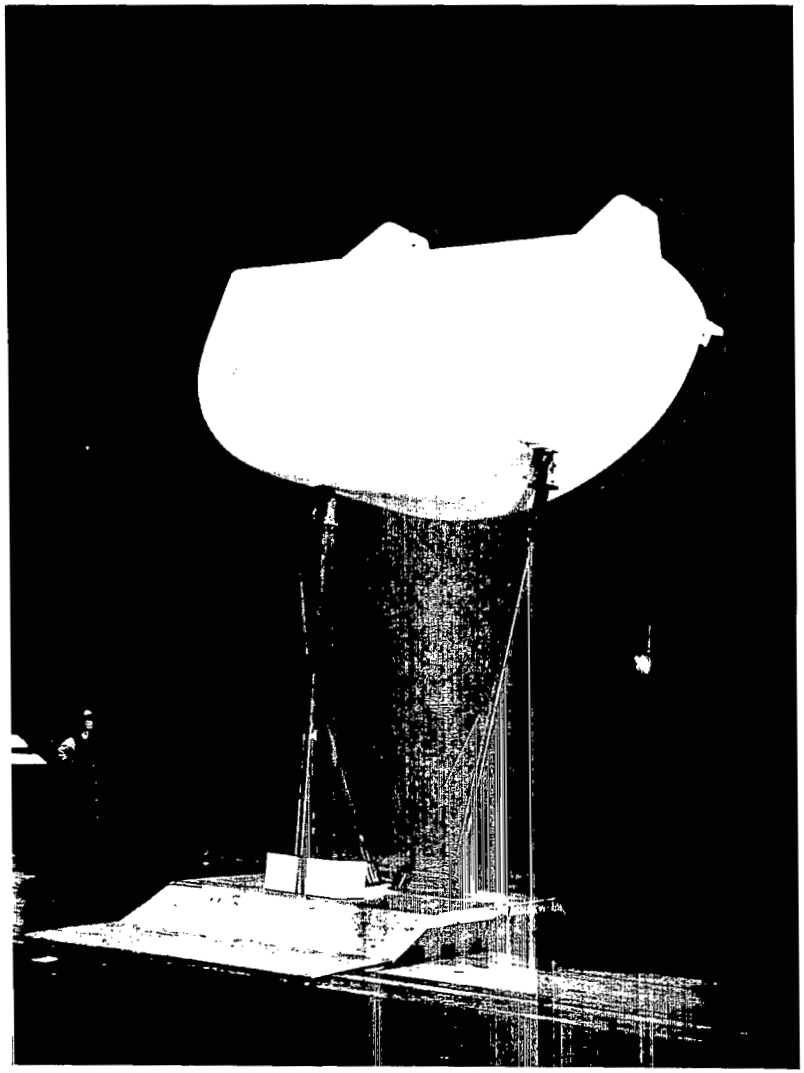

A-30945.1

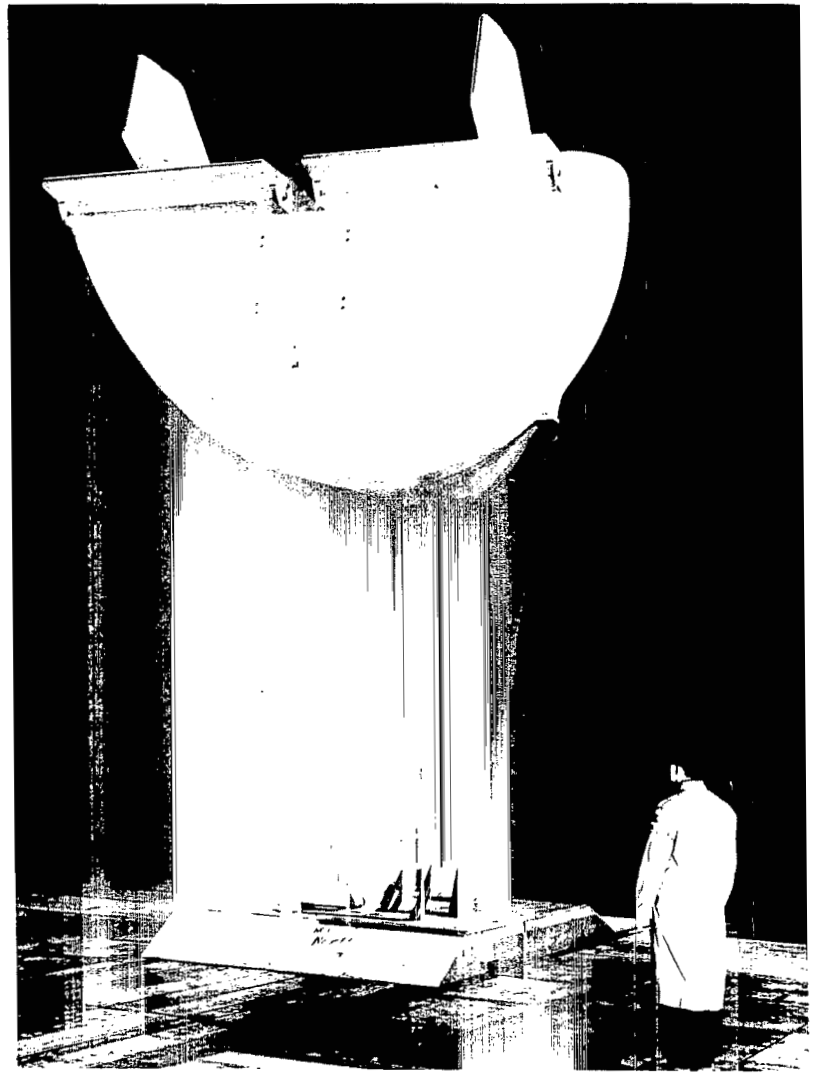

A-30946.1

(b) Model with rigid afterbody.

Figure 1.- Concluded.

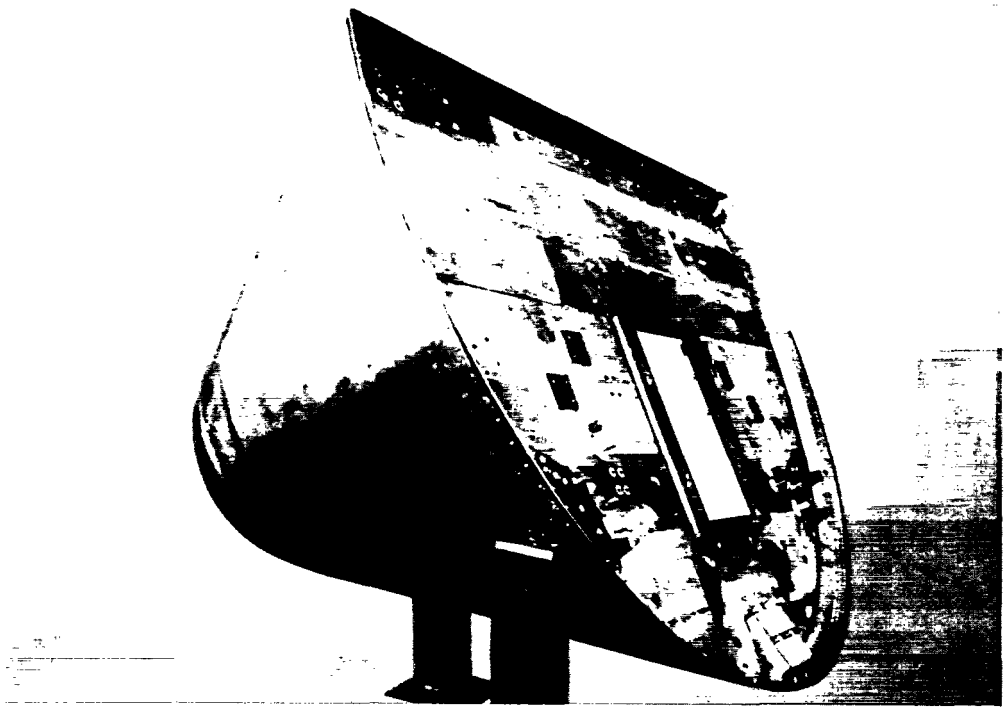

(a) Forebody.

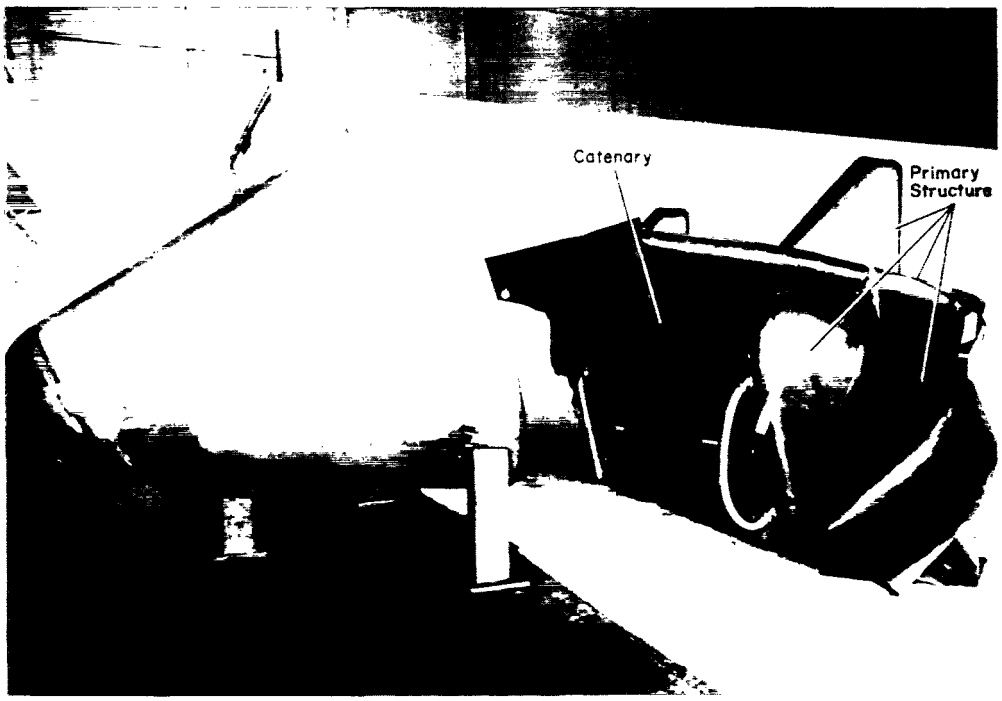

(b) Forebody and inflatable afterbody.

Figure 2.- Model with inflatable afterbody in various stages of assembly.

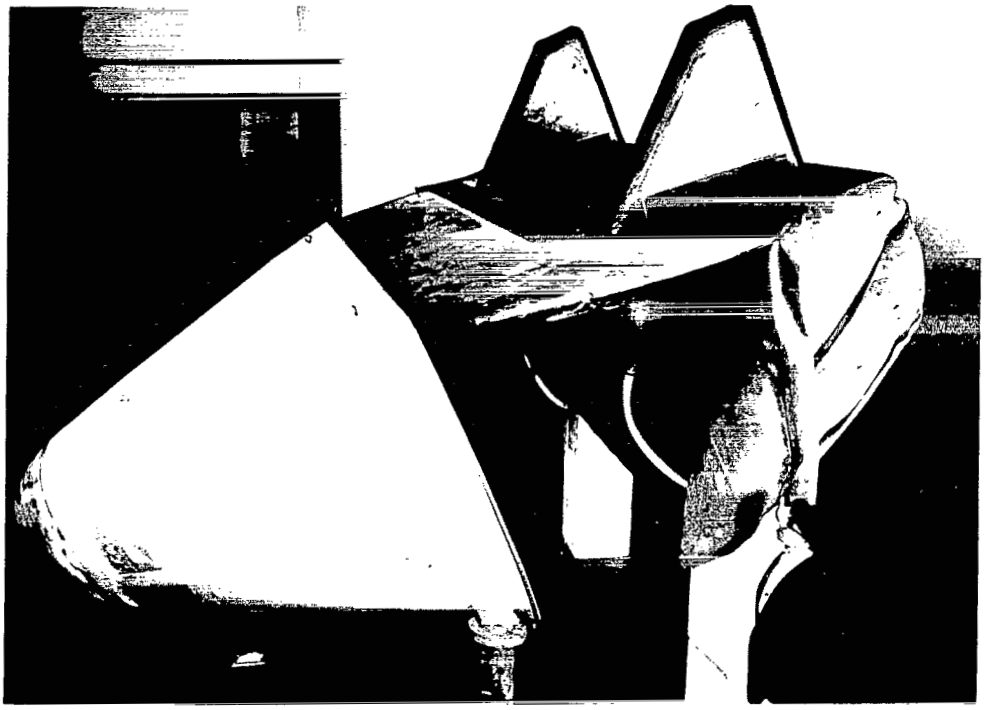

(c) Afterbody attached to forebody.

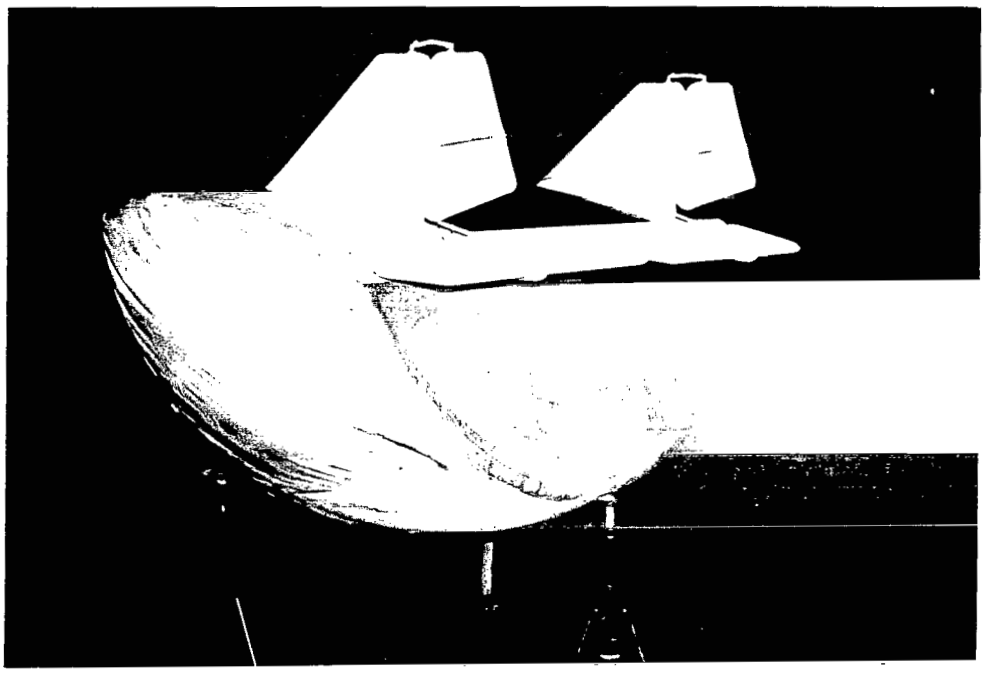

(d) Model assembled with controls.

Figure 2.- Concluded.

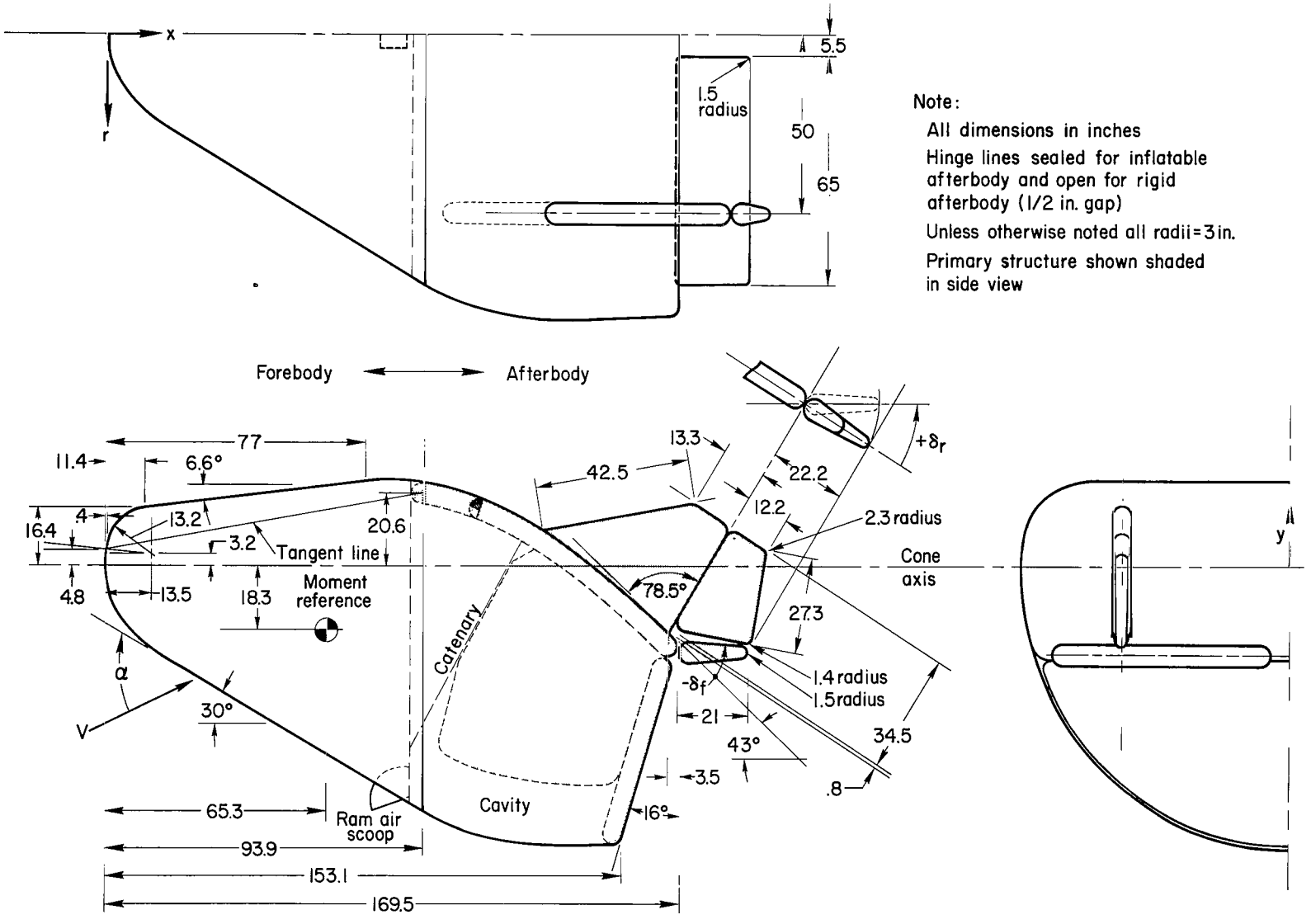

Figure 3.- Basic model dimensions.

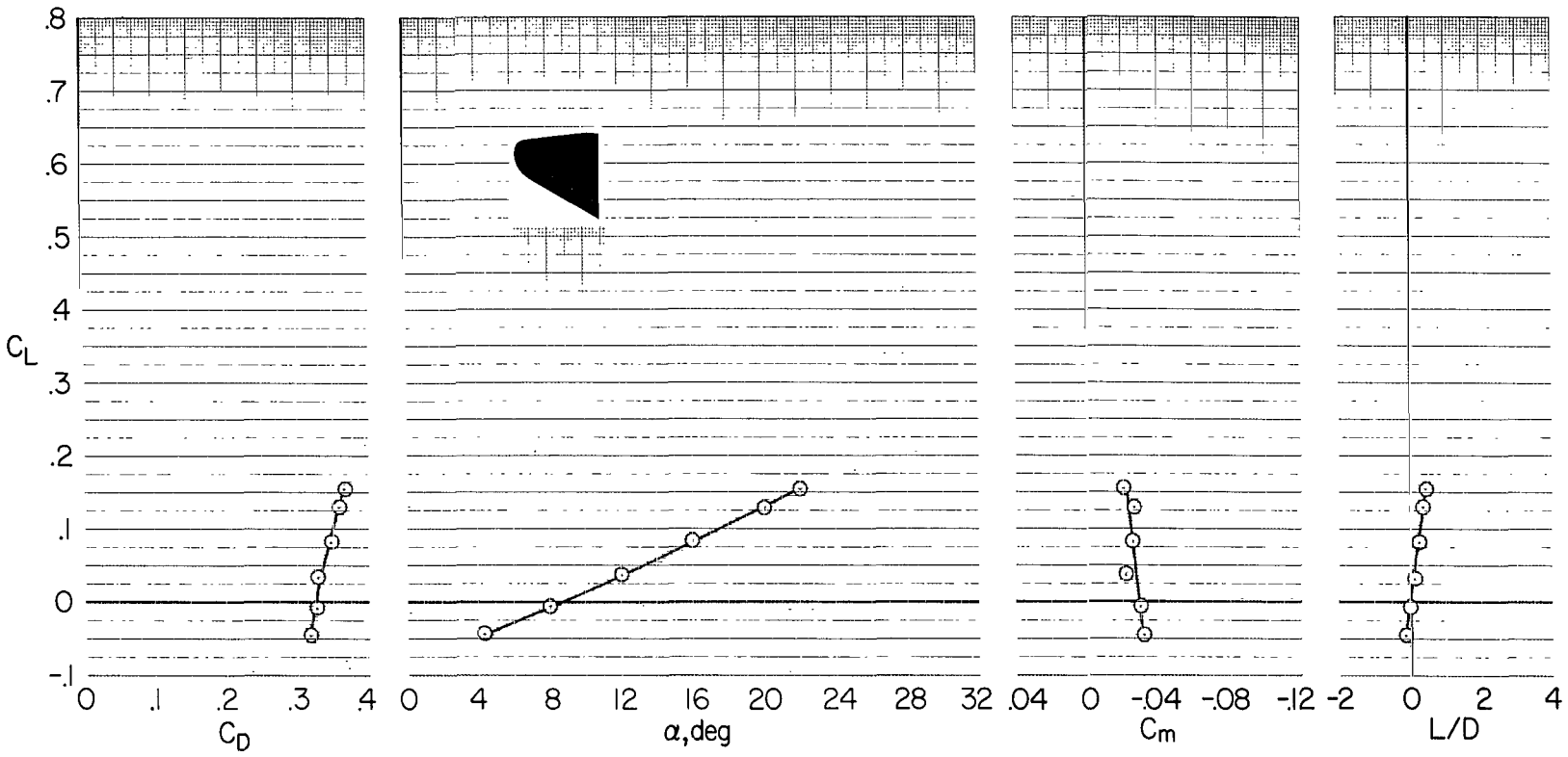

Figure 4.- Aerodynamic characteristics without the afterbody at q = 50 psf.

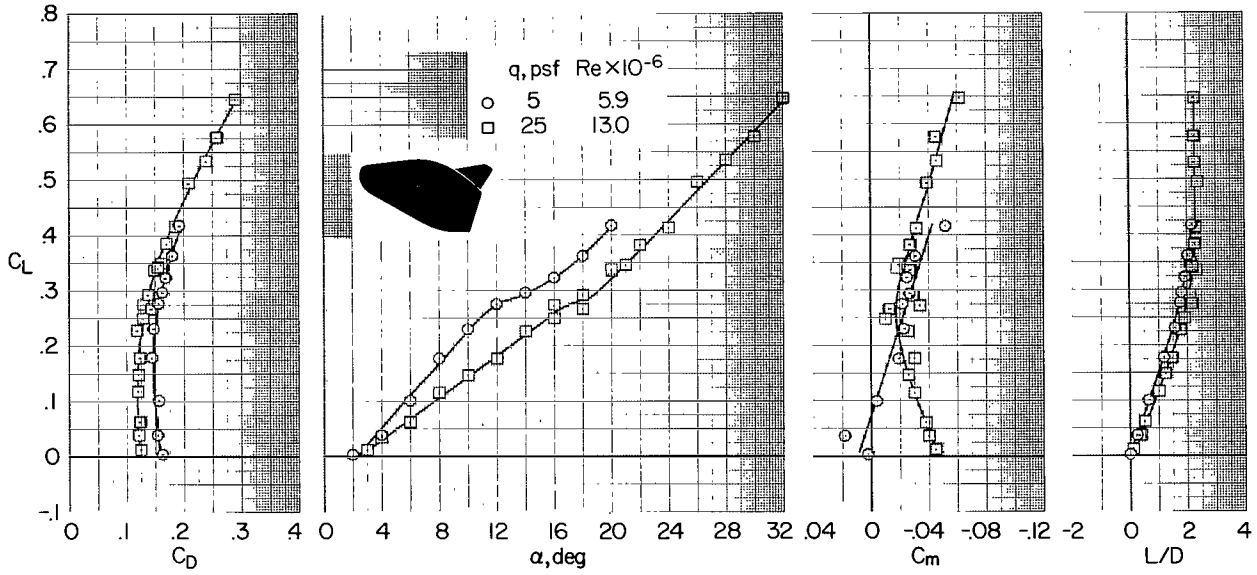

(a) Δp_i = 5 psi and Δp_c = 0.2 psi.

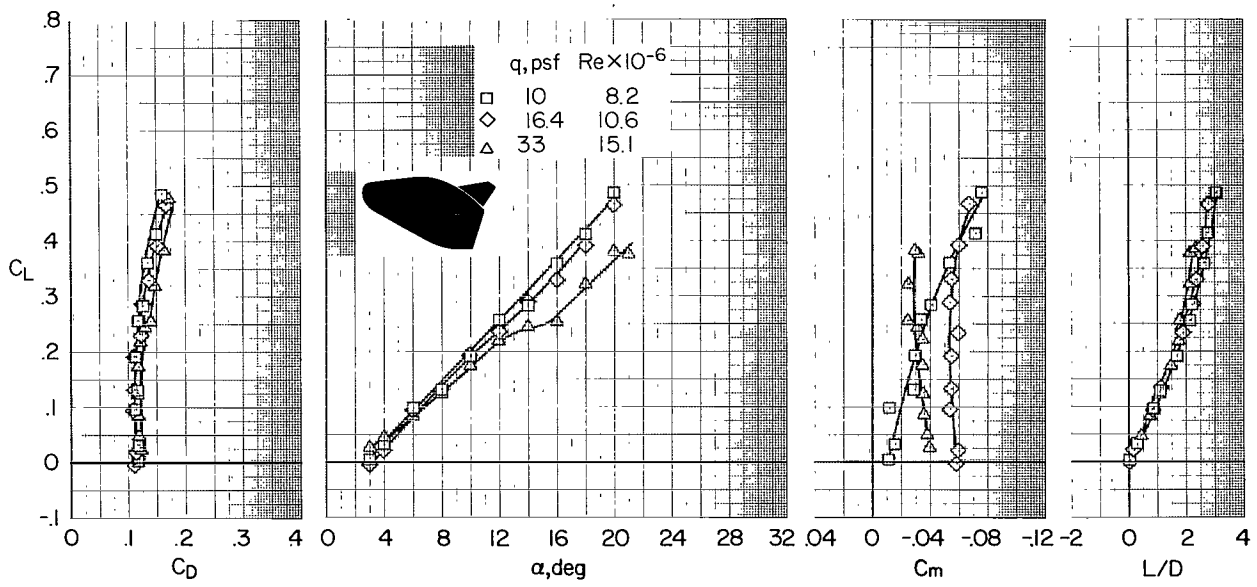

(b) Δp_i = 10 psi and Δp_c = 0.2 psi.

Figure 5.- Aerodynamic characteristics with the inflatable afterbody and without the control surfaces.

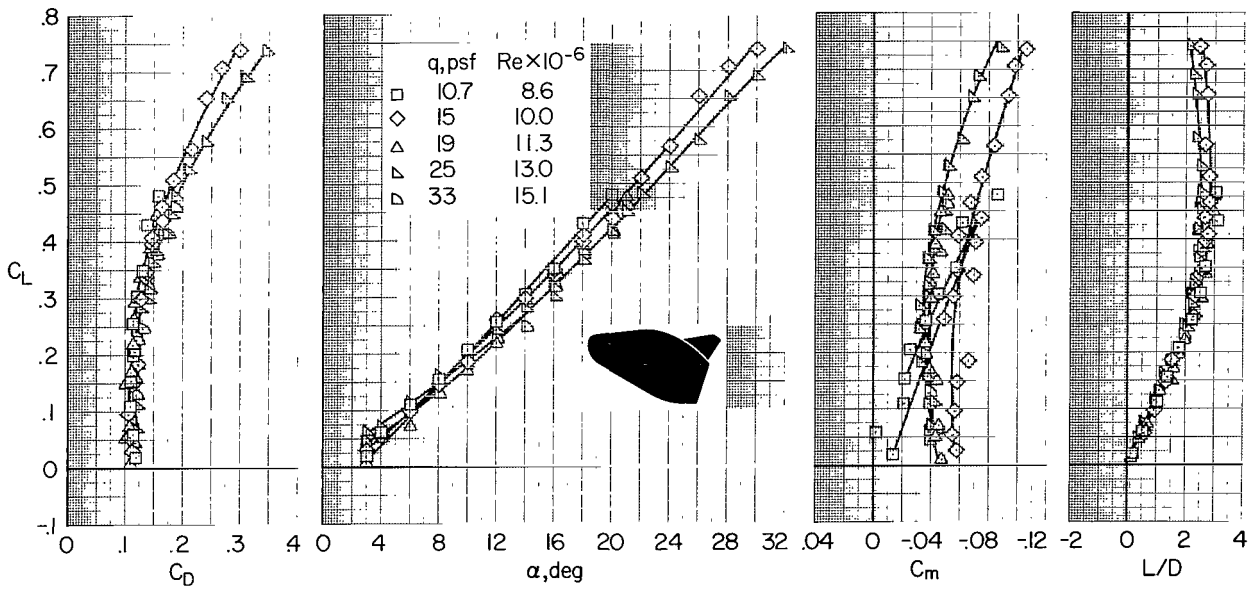

(c) Δp_i = 15 psi and Δp_c = 0.2 psi.

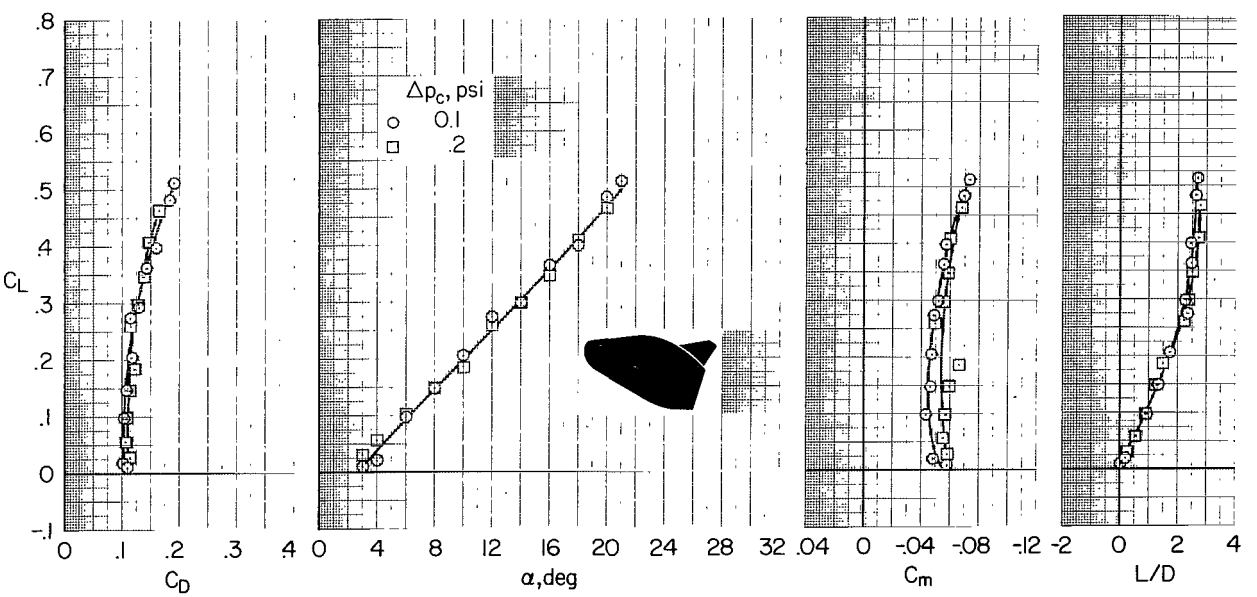

(d) Δp_i = 15 psi and q = 15 psf.

Figure 5.- Concluded.

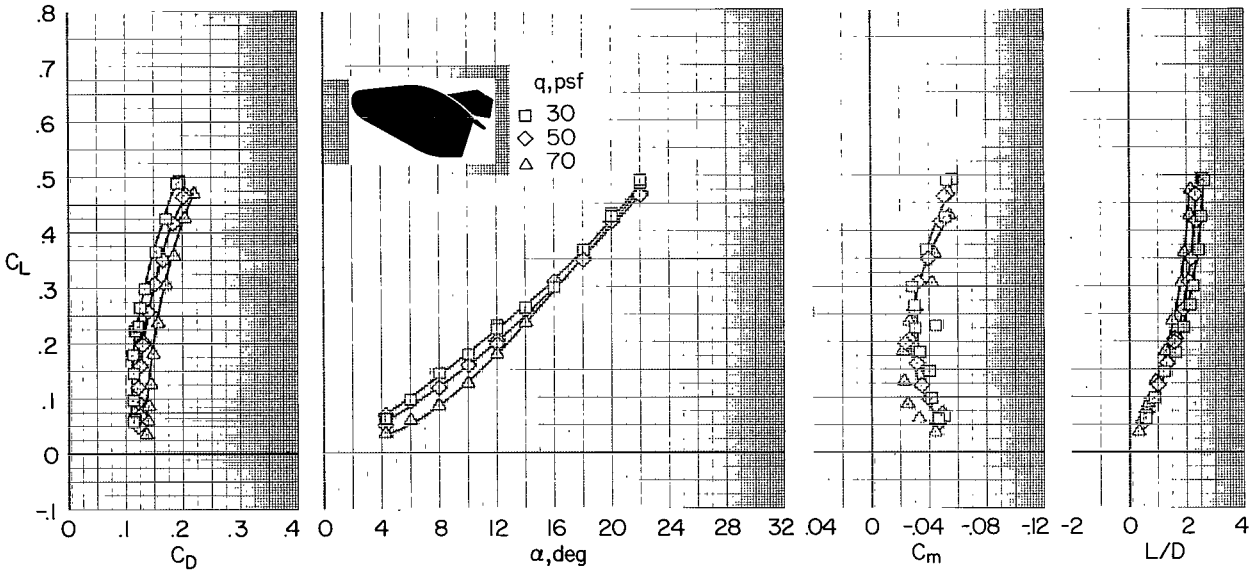

Figure 6.- Aerodynamic characteristics with the inflatable afterbody and with inflatable control surfaces at $\delta_f = 0°$ and $\delta_r = 0°$; $\Delta p_i = 15$ psi, $\Delta p_c = 0.2$ psi.

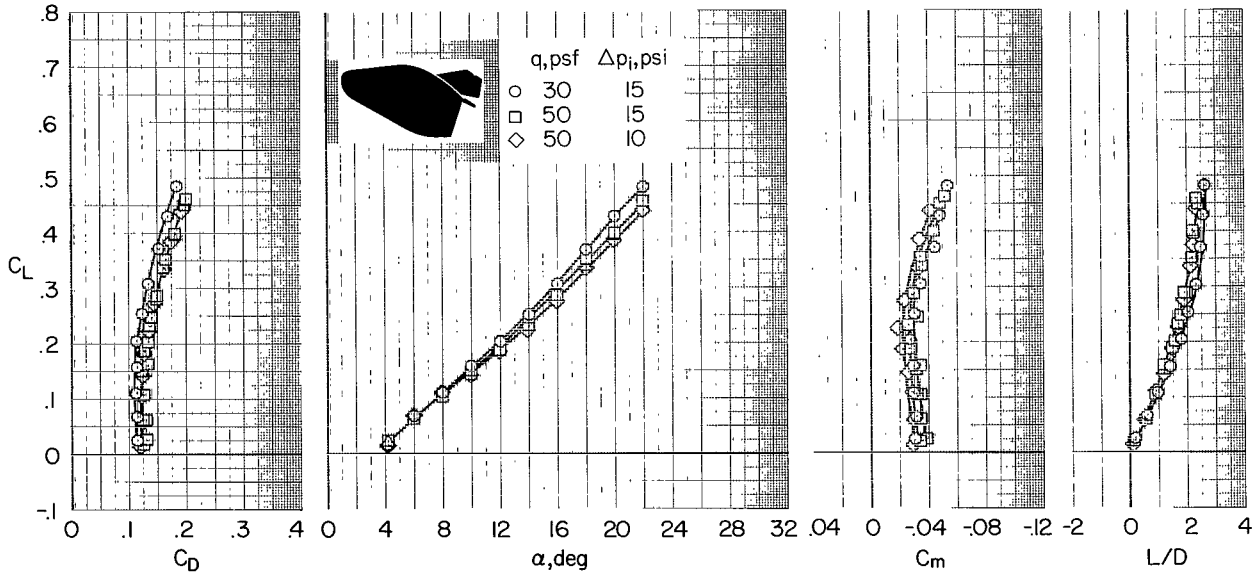

(a) $\Delta p_c = 0.2$ psi.

Figure 7.- Aerodynamic characteristics with the inflatable afterbody and with inflatable control surfaces at $\delta_f = -10°$ and $\delta_r = 0°$.

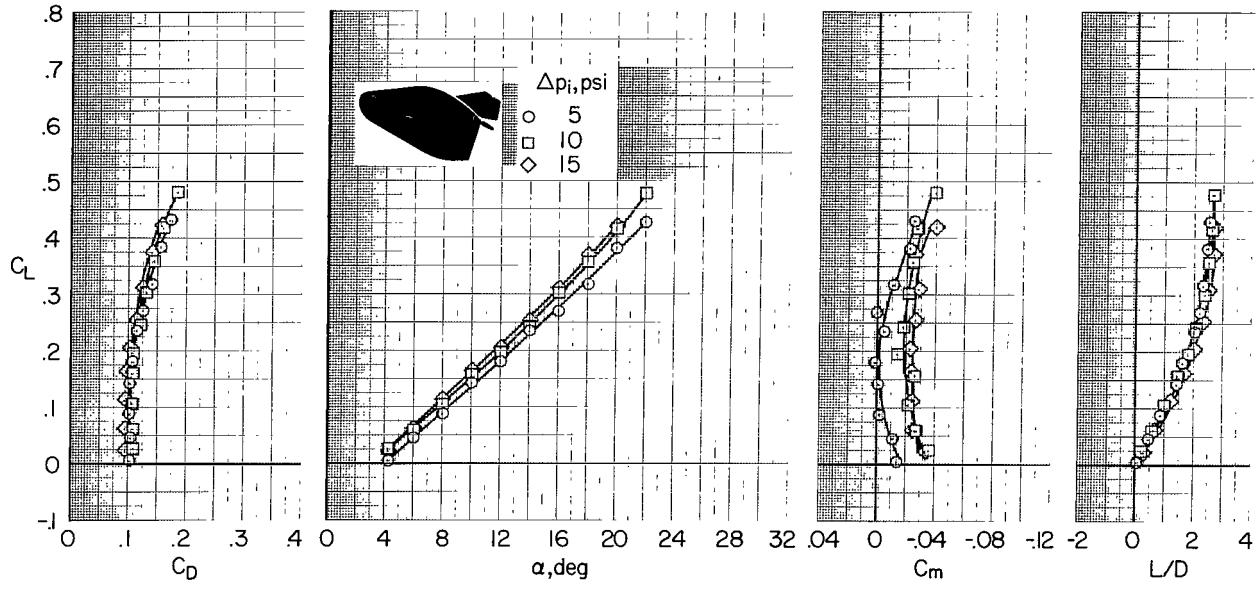

(b) Δp_c = 0.2 psi and q = 15 psf.

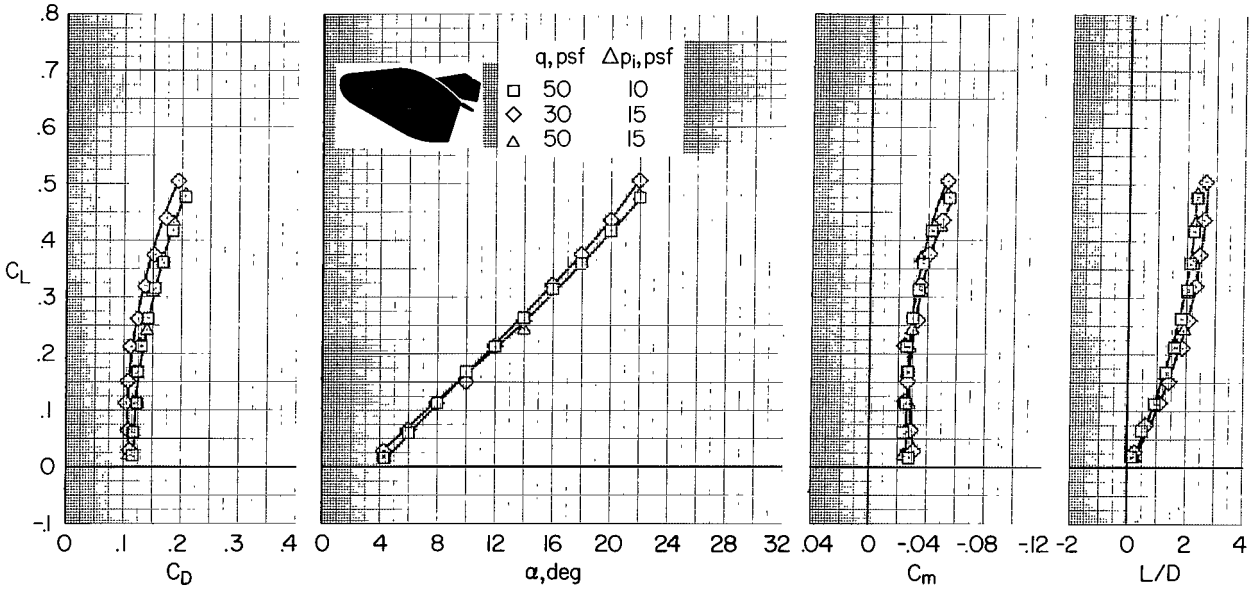

(c) Δp_c = 0.1 psi.

Figure 7.- Concluded.

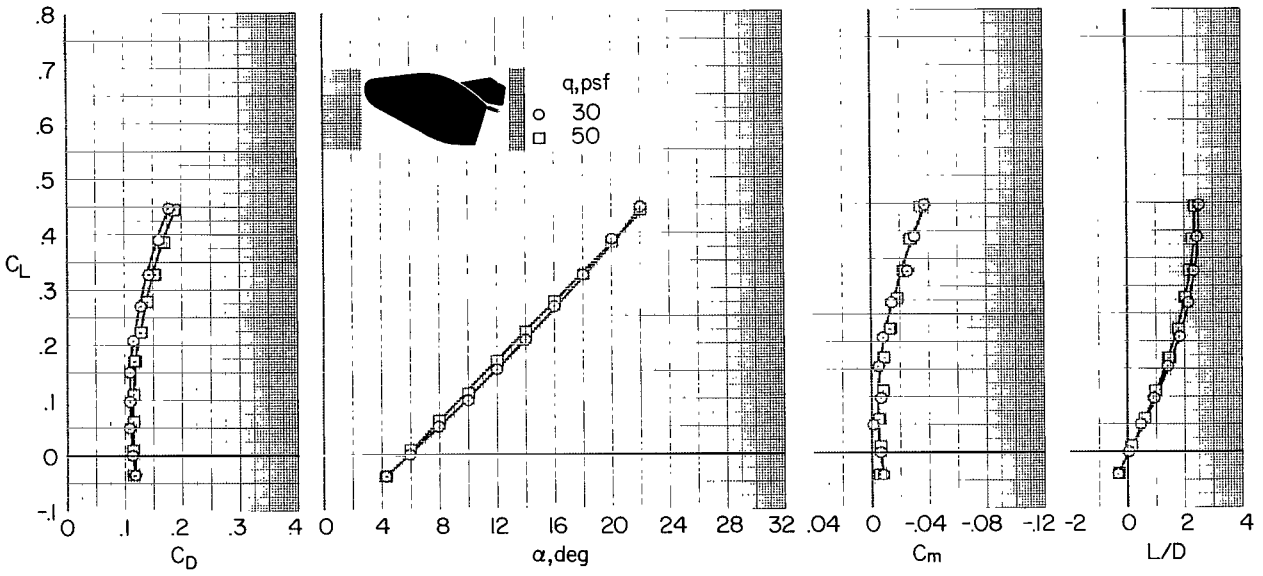

Figure 8.- Aerodynamic characteristics with the inflatable afterbody and with inflatable control surfaces at $\delta_f = -20°$ and $\delta_r = 0°$; $\Delta p_i = 15$ psi, $\Delta p_c = 0.2$ psi.

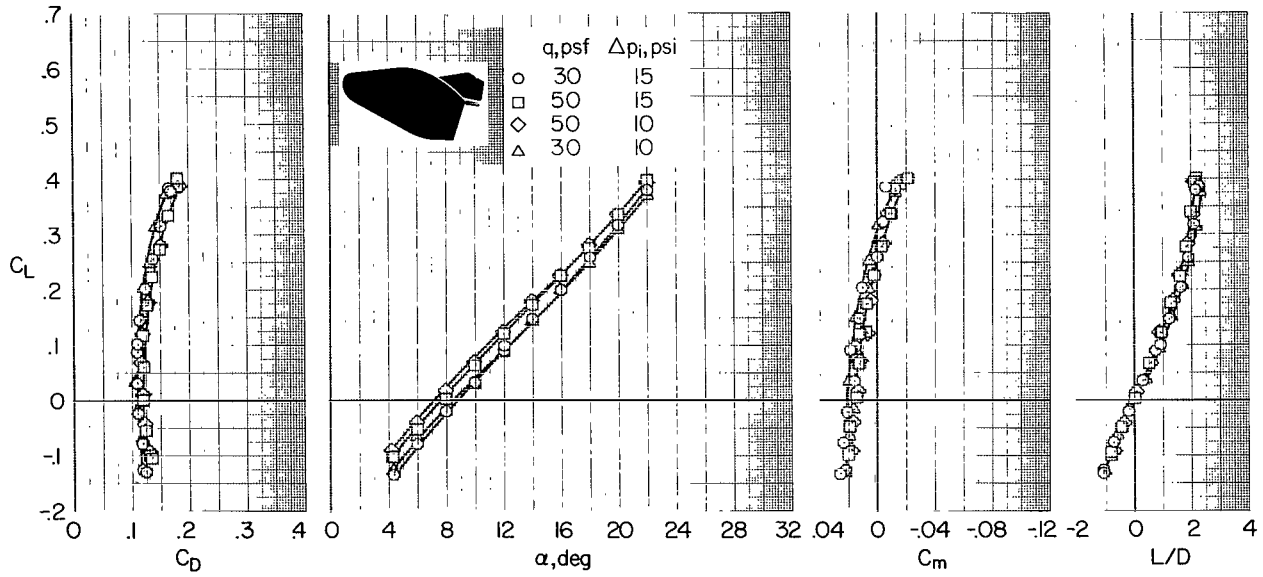

Figure 9.- Aerodynamic characteristics with the inflatable afterbody and with the inflatable control surfaces at $\delta_f = -30°$ and $\delta_r = 0°$; $\Delta p_c = 0.2$ psi.

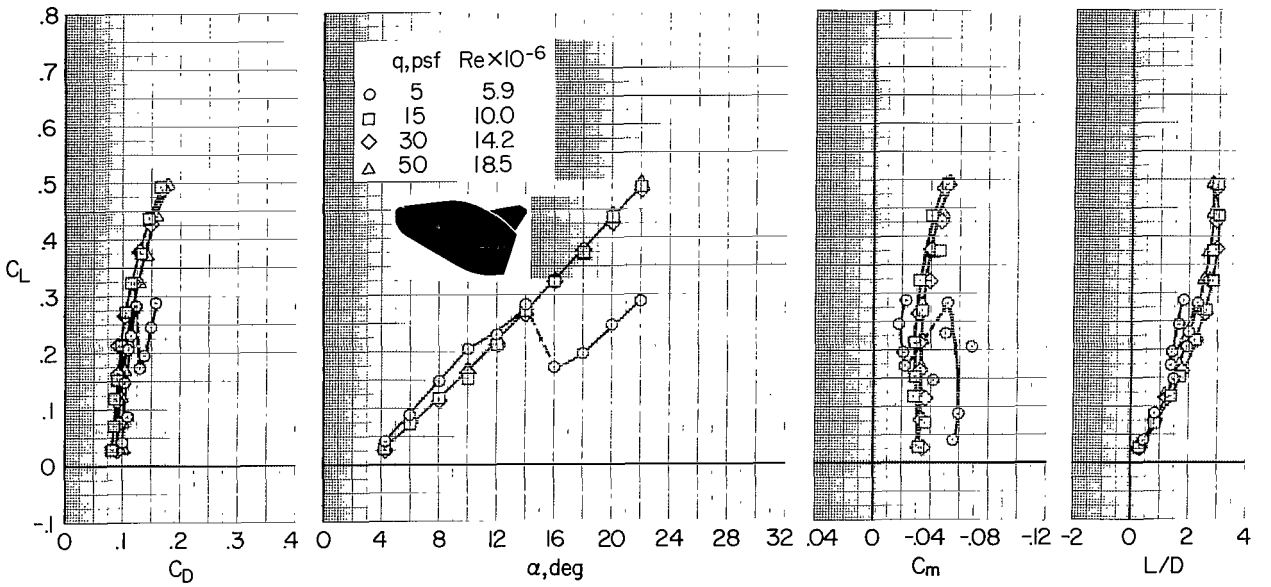

Figure 10.- Aerodynamic characteristics with the rigid afterbody and without control surfaces.

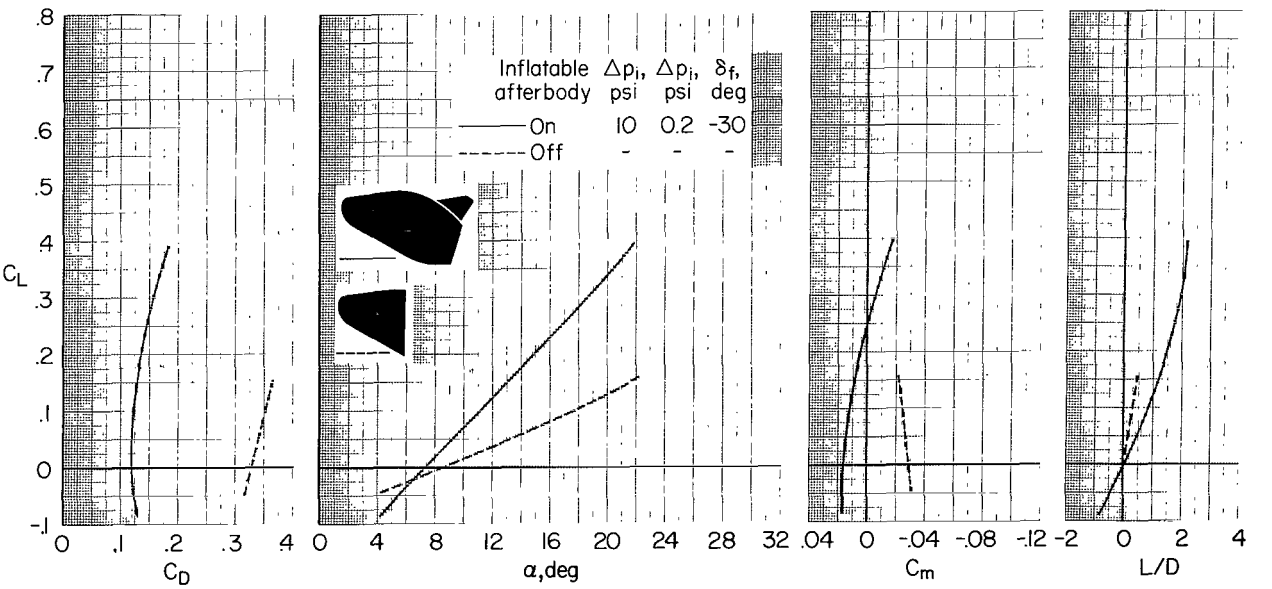

Figure 11.- Comparison of aerodynamic characteristics with and without inflatable afterbody at a dynamic pressure of 50 psf.

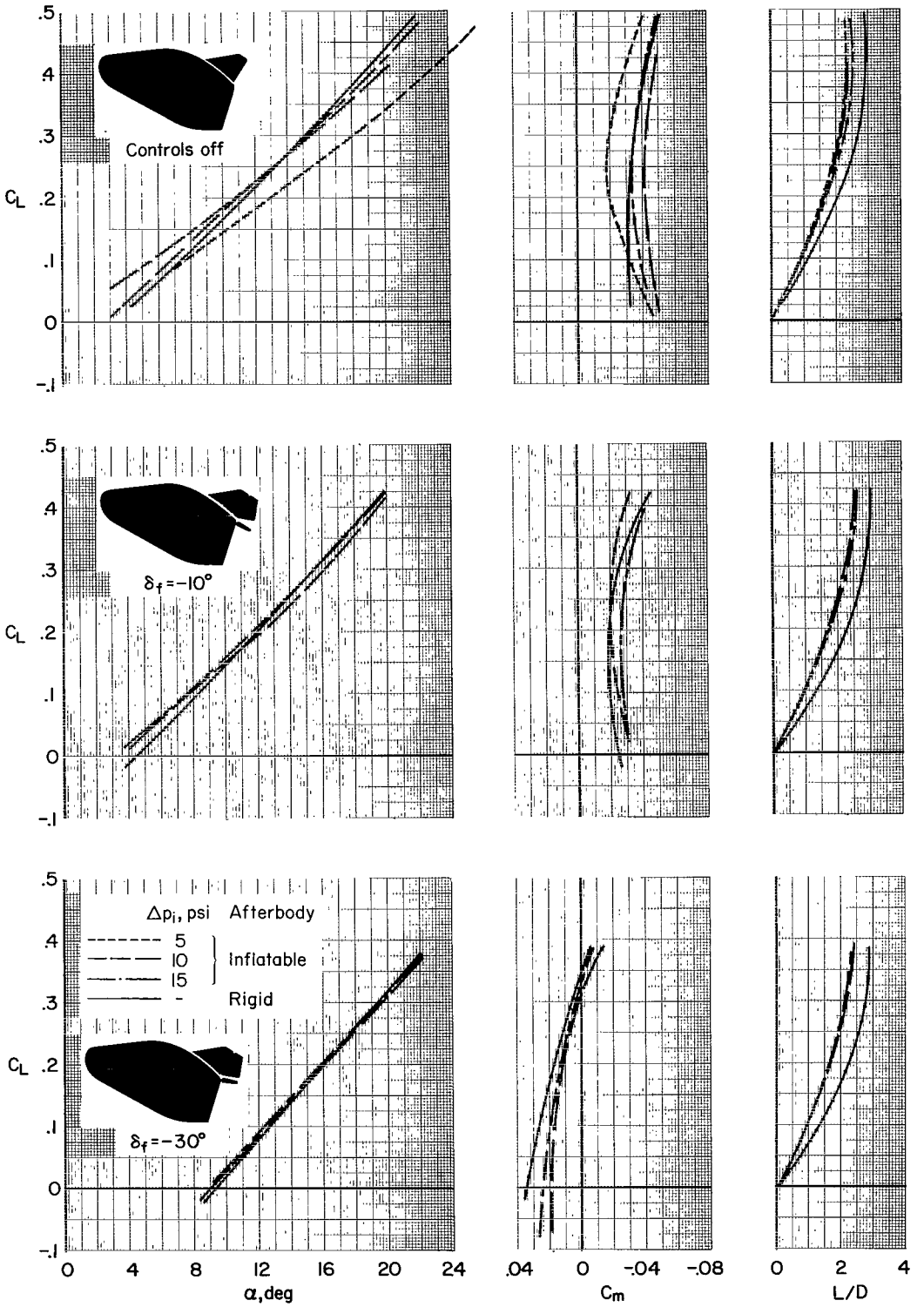

Figure 12.- Comparison of the inflatable configuration with the rigid configuration at a dynamic pressure of 25 psf and Δp_c = 0.2 psi.

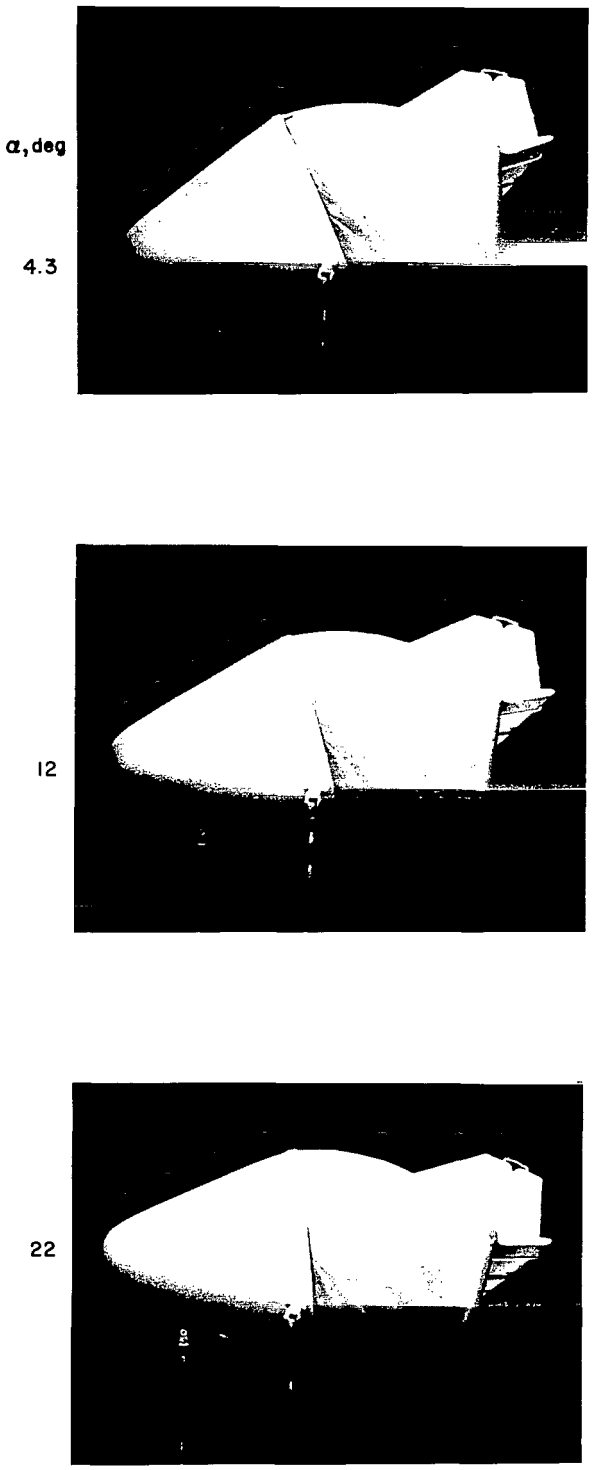

Figure 13.- Model with inflatable afterbody for three angles of attack, a dynamic pressure of 29 psf and an upper flap setting of -30°; Δp_i = 15 psi, Δp_c = 0.2 psi.

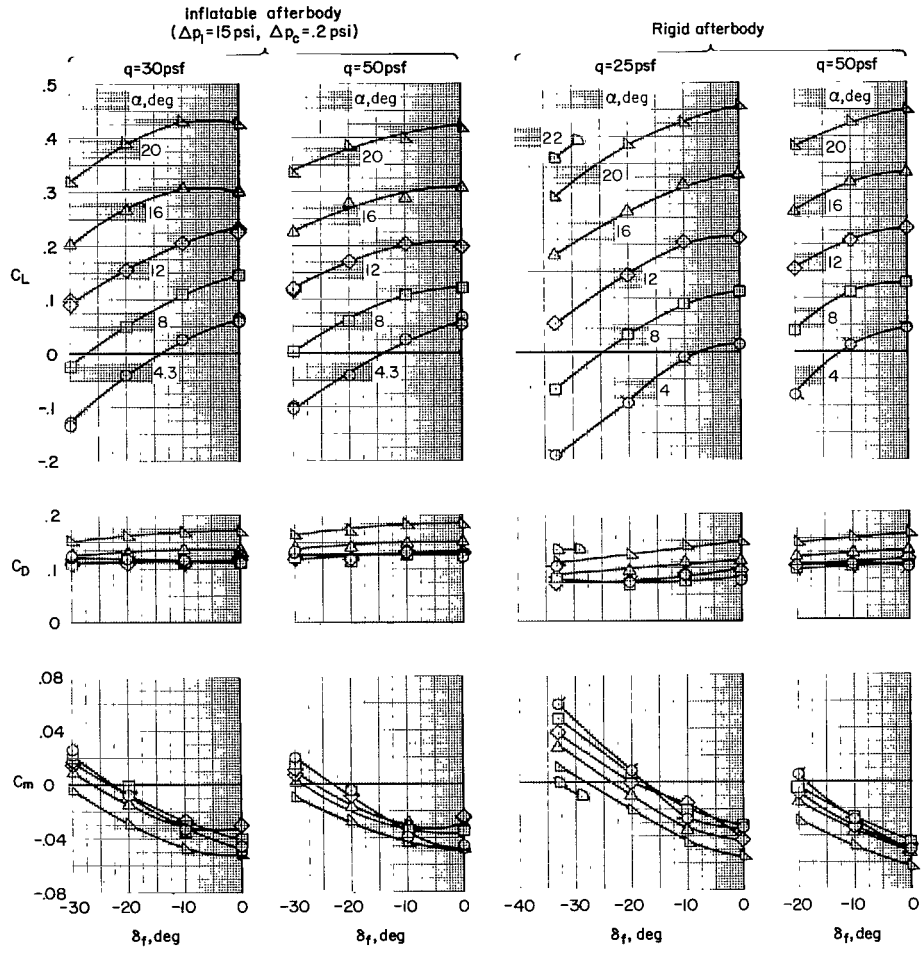

Figure 14.- Effect of flap deflection on the longitudinal aerodynamic characteristics.

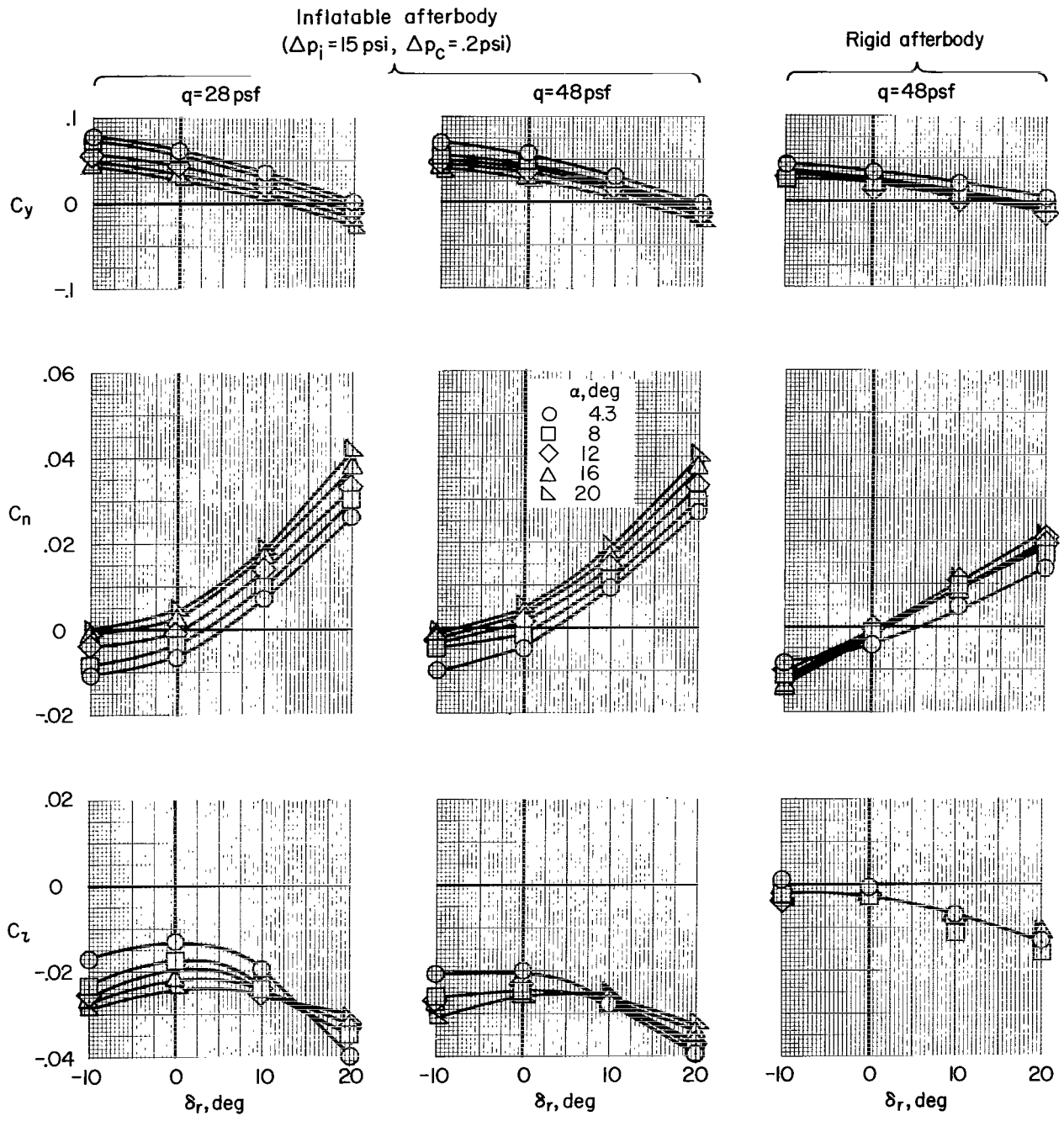

Figure 15.- Effect of rudder deflection on the lateral-directional aerodynamic characteristics.

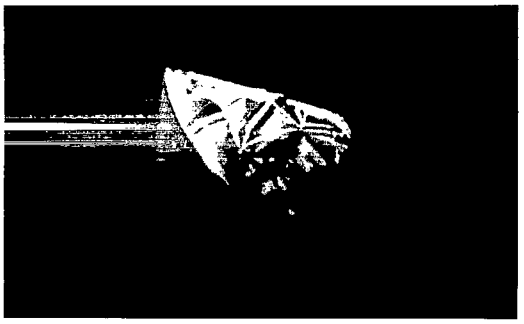

T = 0sec, Δp_i = 0psi, Δp_c = 0psi

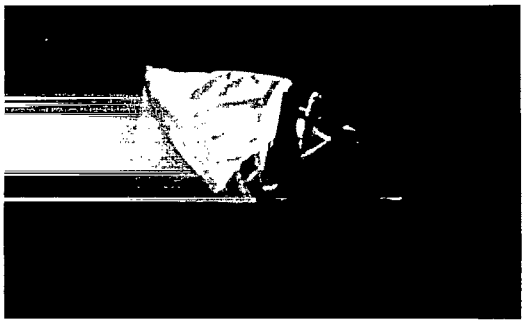

T = 0.7sec, Δp_i = 0psi, Δp_c = 0psi

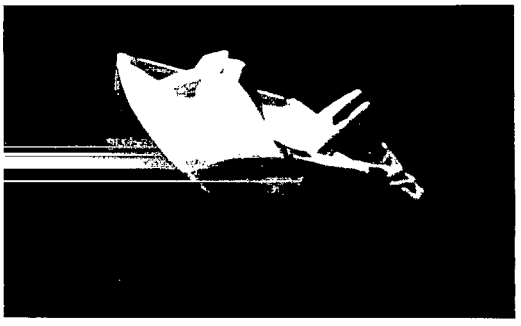

T = 1.3sec, Δp_i = 0psi, Δp_c = 0psi

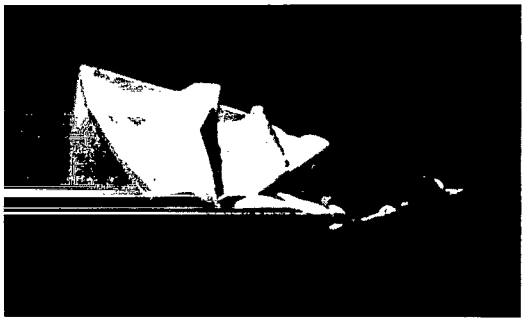

T = 2.3sec, Δp_i = 0psi, Δp_c = 0psi

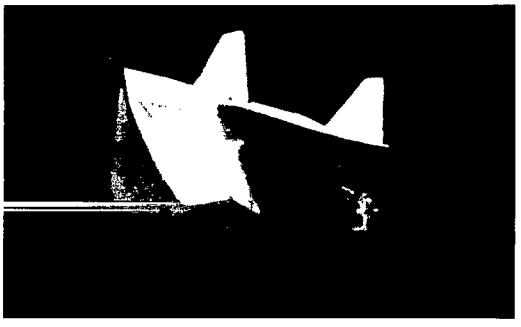

T = 4.0sec, Δp_i = 4.8psi, Δp_c = 0psi

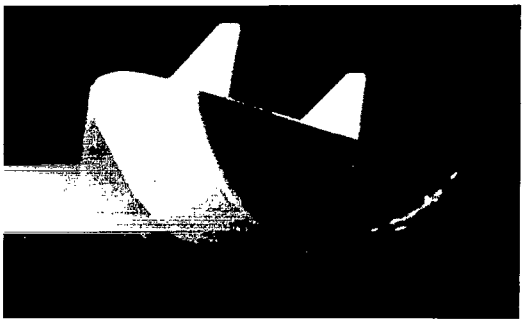

T = 10.0sec, Δp_i = 14psi, Δp_c = .02psi

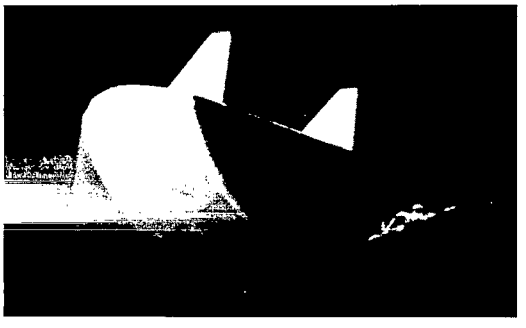

T = 60.0sec, Δp_i = 20psi, Δp_c = .05psi

(a) q = 24 psf, controls off.

Figure 16.- Deployment.

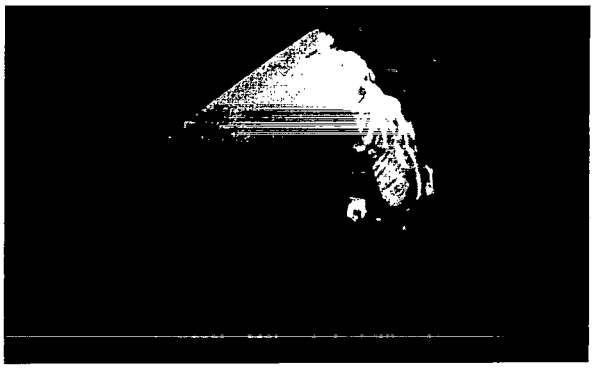

T = 0 sec, Δp_i = 0 psi, Δp_c = 0 psi

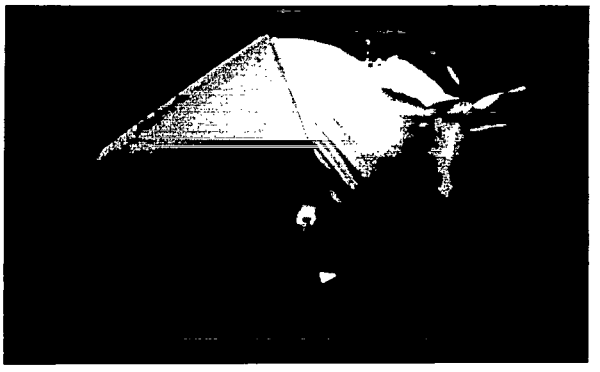

T = 1 sec, Δp_i = 0 psi, Δp_c = .01 psi

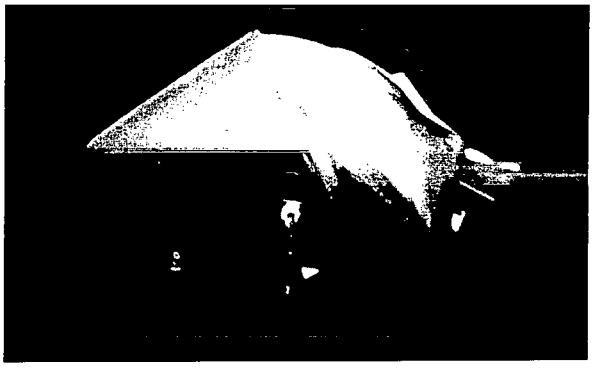

T = 1.5 sec, Δp_i = 0 psi, Δp_c = .01 psi

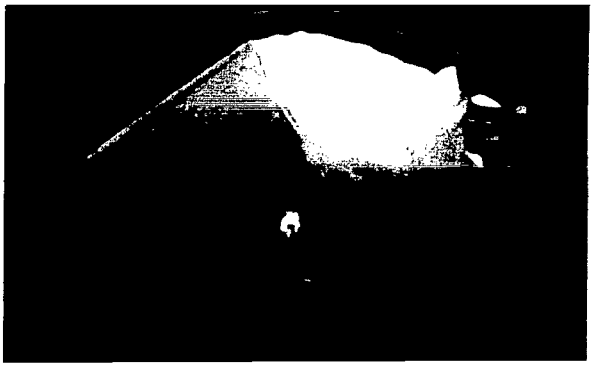

T = 3.1 sec, Δp_i = 0 psi, Δp_c = .11 psi

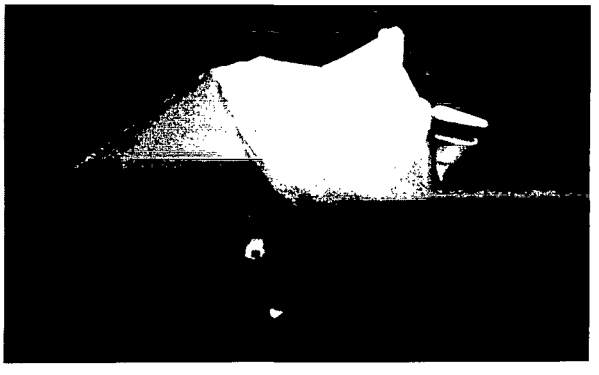

T = 21.2 sec, Δp_i = 0 psi, Δp_c = .12 psi

(b) q = 62 psf, flaps on.

Figure 16.- Concluded.

NASA-Langley, 1969 —— 1 A-2894

NATIONAL AERONAUTICS AND SPACE ADMINISTRATION
WASHINGTON, D. C. 20546

OFFICIAL BUSINESS

FIRST CLASS MAIL

POSTAGE AND FEES PAID
NATIONAL AERONAUTICS AND
SPACE ADMINISTRATION

"The aeronautical and space activities of the United States shall be conducted so as to contribute . . . to the expansion of human knowledge of phenomena in the atmosphere and space. The Administration shall provide for the widest practicable and appropriate dissemination of information concerning its activities and the results thereof."

—NATIONAL AERONAUTICS AND SPACE ACT OF 1958

NASA SCIENTIFIC AND TECHNICAL PUBLICATIONS

TECHNICAL REPORTS: Scientific and technical information considered important, complete, and a lasting contribution to existing knowledge.

TECHNICAL NOTES: Information less broad in scope but nevertheless of importance as a contribution to existing knowledge.

TECHNICAL MEMORANDUMS: Information receiving limited distribution because of preliminary data, security classification, or other reasons.

CONTRACTOR REPORTS: Scientific and technical information generated under a NASA contract or grant and considered an important contribution to existing knowledge.

TECHNICAL TRANSLATIONS: Information published in a foreign language considered to merit NASA distribution in English.

SPECIAL PUBLICATIONS: Information derived from or of value to NASA activities. Publications include conference proceedings, monographs, data compilations, handbooks, sourcebooks, and special bibliographies.

TECHNOLOGY UTILIZATION PUBLICATIONS: Information on technology used by NASA that may be of particular interest in commercial and other non-aerospace applications. Publications include Tech Briefs, Technology Utilization Reports and Notes, and Technology Surveys.

Details on the availability of these publications may be obtained from:

SCIENTIFIC AND TECHNICAL INFORMATION DIVISION

NATIONAL AERONAUTICS AND SPACE ADMINISTRATION

Washington, D.C. 20546